Catalysis Science & Technology

ROYAL SOCIETY OF CHEMISTRY

PAPER

View Article Online
View Journal | View Issue

Cite this: *Catal. Sci. Technol.*, 2020, **10**, 5245

Aqueous phase reforming of xylitol and xylose in the presence of formic acid

Matias Alvear,[a] Atte Aho,[a] Irina L. Simakova,[b] Henrik Grénman,[a] Tapio Salmi[a] and Dmitry Yu. Murzin *[a]

Received 21st April 2020,
Accepted 2nd July 2020

DOI: 10.1039/d0cy00811g

rsc.li/catalysis

Aqueous phase reforming (APR) of xylose and xylitol was studied over Pt/Pd catalysts supported on mesoporous carbon (Sibunit) in the temperature range 175–225 °C in a laboratory-scale packed bed reactor. Formic acid was introduced to the reaction mixture to simulate an industrial feedstock from the reactive extraction of hemicelluloses from biomass. The conversion was higher in xylose APR, however, xylitol APR displayed a higher selectivity to hydrogen and stable operation under the conditions investigated. Addition of formic acid increased the hydrogen production in the APR of xylitol, while xylose APR displayed an opposite behavior. The ratio of the gas and liquid products was similar for both substrates at an equal conversion, however, the alkane distribution was different, depending on the presence of formic acid and reaction temperature. It can be concluded that the APR of xylitol to hydrogen was successfully conducted with the selected catalyst in the presence of formic acid as a co-reactant.

1. Introduction

Aqueous phase reforming (APR) has been widely studied employing different heterogeneous catalysts and substrates such as various alcohols and polyols.[1–12] APR of xylitol in particular has been addressed in the literature for the production of hydrogen and alkanes.[13–23] Aqueous phase reforming of xylose,[23–25] in contrast, has been scarcely investigated and is typically mentioned just as an intermediate in the reaction pathway towards the APR of xylitol and sorbitol.[17,26] Kirilin *et al.* reported detailed screening of mono- and bimetallic catalysts with different supports in the APR of xylitol.[14–18] Platinum displayed the best selectivity to hydrogen among the monometallic catalysts. Kirilin *et al.*[16] and Godina *et al.*[14] reported that the catalyst acidity influences the selectivity to hydrogen significantly. The catalyst stability was observed to depend on the support during long-term experiments and carbon-based catalysts were concluded to be a good option as they are stable also at higher temperatures under hydrothermal conditions.[15]

Murzin *et al.*[17] studied aqueous-phase reforming of xylitol over a Pt/C catalyst at 225 °C, 30 bar and varying residence times, obtaining an average selectivity to hydrogen between 80 and 90%, with a turnover frequency (TOF) between 3 and 9.3 min^{-1}. Alkanes and carbon monoxide were produced as side products with a 10% selectivity. Moreover, detailed overall process design incorporating the reaction kinetics was, for the first time in the open literature, described for the APR of xylitol.[17] The kinetic model was able to account for both the liquid and gas phase products. It was suggested that the gas phase by-products (alkanes) could be used as a fuel for reactor heating, allowing efficient heat integration.

APR of xylitol requires hydrogenation of xylose as the first step, which is typically performed at lower temperatures (~120 °C). Performing the hydrogenation in a separate step prior to the APR decreases the techno-economic viability of the overall process.

Formic acid can be successfully used in biomass fractionation according to the literature[27–33] giving hemicelluloses which can be further hydrolysed to monomeric sugars. For example, fractionation of woody biomass such as birch can be performed in the presence of formic acid yielding mainly xylose. After such a fractionation step, the downstream APR of xylose or xylitol must be performed in the presence of formic acid. Formic acid decomposition in the presence of supported catalysts has been widely studied[34–39] and palladium has been observed to be an efficient metal for this purpose. Moreover, palladium has also been used for APR *per se* with reasonably good results.[40–42] The reason for selecting carbon as a support is related to the absence of transformations under hydrothermal conditions contrary for example to alumina and a possibility to regenerate the catalyst upon treatment with hydrogen as reported previously.[43]

[a] *Laboratory of Industrial Chemistry and Reaction Engineering, Johan Gadolin Process Chemistry Centre, Åbo Akademi University, Turku/Åbo, 20500, Finland. E-mail: dmurzin@abo.fi*
[b] *Boreskov Institute of Catalysis, pr. Lavrentieva, 5, 630090, Novosibirsk, Russia*

The current work focuses on investigating whether carbon supported bimetallic Pt/Pd catalyst can be used in the APR of xylose solutions containing formic acid. The latter as mentioned above is applied in an upstream step of reactive hemicelluloses (*e.g.* xylan) hydrolysis. The hypothesis is that formic acid can be decomposed and a reductive atmosphere will contribute to *in situ* hydrogenation of xylose to xylitol allowing successful APR of the sugar and avoiding typically encountered formation of humins reported in a wide range of conditions in the literature for different sugars, for example glucose.[44–46]

APR of xylitol *per se* and in the presence of formic acid was investigated in the current work not only for the sake of comparison, but also to explore the feasibility of APR for a mixture of xylitol and formic acid. Such a mixture is formed when xylose, generated in reaction extraction combined with hydrolysis, is subsequently hydrogenated.

2. Experimental

2.1. Chemicals

$PdCl_2$ (Kraszvetmet, Krasnoyarsk, Russia) and H_2PtCl_6 (Kraszvetmet, Krasnoyarsk, Russia) were utilized as catalyst precursors. Mesoporous carbon Sibunit (S_{BET} = 350 m^2 g^{-1}, fraction 200 ÷ 500 μm) was used as a support. The compounds utilized in this work were xylose (Sigma-Aldrich, 99%) and xylitol (Sigma-Aldrich, 99%).

2.2. Catalyst and catalyst preparation

The catalyst contained 2.50 wt% Pt and 0.6 wt% Pd supported on the mesoporous carbon Sibunit. The catalyst was prepared by incipient wetness impregnation with a solution of H_2PtCl_6 (0.1 M) and $PdCl_2$ (0.1 M). Thereafter, the samples were desiccated for 17 hours at 110 °C and reduced by molecular hydrogen by gradually increasing the temperature from room temperature to 400 °C at a ramping rate of 2 °C min^{-1}. Moreover, for eliminating the excess chloride the samples were treated with hydrogen for 3 h at 400 °C.

2.3. Catalyst characterization

The metal dispersion of the catalyst was determined by CO chemisorption using Micromeritics 2910 AutoChem equipment. The CO-to-metal ratio was assumed to be unity in the interpretation of the results. The catalyst was reduced at 250 °C under a flow of hydrogen before the CO chemisorption at 25 °C.

Leo 1530 Gemini and Jeol JEM-1400Plus microscopes were used to obtain the scanning (SEM) and transmission electron micrographs (TEM) of the catalysts, respectively.

A scanning electron microscope (SEM) coupled with an energy dispersive X-ray analyzer (EDXA) was utilized to obtain information on the elemental analysis and metal distribution of the catalyst. An acceleration voltage of 15 kV was used for the X-ray analyzer. To obtain a high quality image and enhance the conductivity, the catalyst was placed as a thin layer on top of the carbon coating.

For TEM the maximal acceleration voltage was 120 kV. Interpretation of TEM images and determination of the particle sizes were done using the ImageJ program.

2.4. Set-up

The setup used during the catalytic experiments is illustrated in Fig. 1. A 3% aqueous solution of the substrate was fed along with nitrogen containing 1% helium through a trickle bed reactor with an internal diameter of 4.6 mm and length of 50 cm. The catalyst bed was composed of 2.50 wt% Pt and 0.6 wt% Pd supported on mesoporous carbon Sibunit (0.534 g) and glass beads in a weight proportion of 1 : 6. A HPLC pump (Elmex 1SM) was utilized for the liquid-phase feed while the gas phase was fed through a flow controller (MFC-1). A pressure controller (PC-1) was installed downstream the reactor. An Equilibar U3L ultra low flow back pressure regulator was utilized to control the pressure. Further

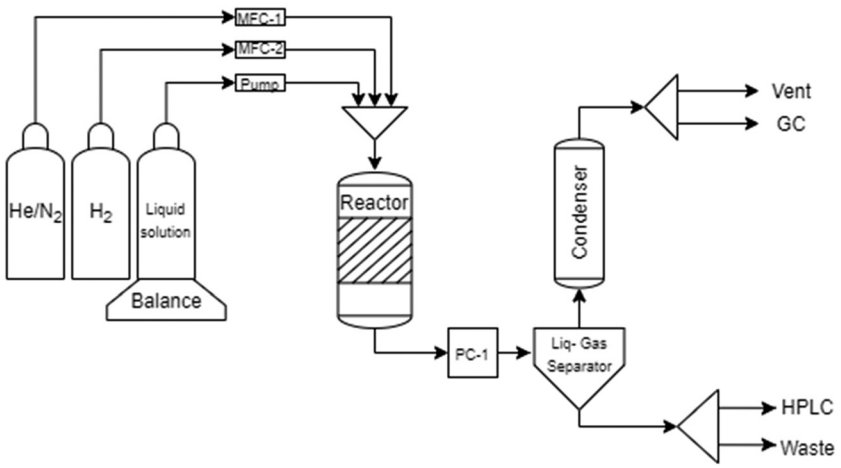

Fig. 1 Experimental set-up for aqueous phase reforming.

Table 1 Gases calibrated in the micro GC

Gases					
Carbon dioxide	Iso-butane	Iso-pentane	*n*-Hexane	Helium	Methane
Ethylene	*n*-Butane	*n*-pentane	Cyclic hexane	Hydrogen	Carbon monoxide
Propylene	Neo-pentane	Iso-hexane	*n*-Heptane	Nitrogen	—

downstream, a gas–liquid separator of 50 mL was operated at room temperature and atmospheric pressure. Liquid chromatography (Hewlett Packard series 1100) was utilized to analyze the liquid samples collected off-line from the separator. More details on the analysis are given below. To prevent clogging of the micro-gas chromatograph (Agilent 3000A), the gas phase passed through a condenser operated at −5 °C. A small amount of the gas phase was taken to the on-line micro-GC for analysis.

The reduction of the catalyst was performed at 250 °C under a constant flow of hydrogen (30 ml min^{-1}) for 2 hours (Fig. 1). Prior to the reduction the set-up was pressurized with the He/N_2 gas mixture and checked for possible leaks. The desired temperature was reached with a ramp of 5 °C min^{-1} under a hydrogen flow. Prior to the reduction the reactor was pressurized with He/N_2 to avoid leaks and purged.

2.5. Analysis of the products

An Agilent 3000A micro-GC equipped with four columns – Plot U, OV-1, Alumina and Molsieve – was used to analyze the gas phase online. In total, 17 gases were calibrated (Table 1) sampling 10 times each gas. The gases included 12 alkanes with carbon numbers from C1 to C7, hydrogen, carbon monoxide and dioxide, nitrogen and helium as an internal standard.

HPLC analysis was performed offline using a Hewlett Packard series 1100 equipped with an Aminex HPX-87H column and a refractive index detector (RI), under isocratic conditions, with a flow rate of 0.6 mL min^{-1} of 5 mM H_2SO_4 water solution and 45 °C. The calibration was performed for 28 compounds (Table 2). Every compound was calibrated with 1 wt%, 0.5 wt% and 0.25 wt% solutions. For formic acid, a sample with 2 wt% was included. In the case of xylose and xylitol, samples with 3 wt% were also analyzed.

2.6. Catalytic experiments

The experimental matrix was composed of two sets of experiments, carried out in the presence and absence of formic acid. Xylose and xylitol were introduced as 3 wt% solutions and 2% of formic acid was added to the second set of experiments. The flows of liquid and gas were kept constant at 0.1 ml min^{-1} and 36.4 ml min^{-1}, respectively. Three different reaction temperatures were employed for xylose, 175, 200 and 225 °C, and the temperatures 200 and 225 °C for xylitol, due to the lower activity. The pressure was set to 32 bar.

Table 2 Substrates calibrated by HPLC

Substrates			
Furfural	Xylitol	Glycerol	Propane-1,2-diol
Xylose	Erythritol	Formaldehyde	Propane-1,3-diol
Sorbitol	Glycolaldehyde	Formic acid	Acetaldehyde
Dulcitol	Glycolic acid	Acetic acid	Methanol
Arabitol	Lactic acid	Ethylene glycol	Butane-1,2-diol
Ethanol	Isopropanol	Pentane-1,2-diol	1-Butanol
Butyric acid	1-Propanol	Butyraldehyde	Hexane-1,2-diol

The concentration of formic acid was selected based on the experimental data for extraction of hemicelluloses from *e.g.* wood and bamboo.

The reactant conversion X was defined as:

$$X = \frac{\dot{n}_{in} - \dot{n}_{out}}{\dot{n}_{in}} = \frac{c_{in}\dot{V}_{in} - c_{out}\dot{V}_{out}}{c_{in}\dot{V}_{in}} \quad (1)$$

Assuming that the volumetric flow ($\dot{V}$) does not change during the reaction, the conversion can be calculated directly with the concentrations obtained by HPLC analysis of the reaction mixture according to

$$X(\%) = \frac{C_{in} - C_{out}}{C_{in}} \times 100\% \quad (2)$$

where C_{in} and C_{out} are the inlet and outlet concentrations, respectively.

The selectivity to H_2 was calculated as:

$$H_2\ \text{selectivity}(\%) = \frac{\text{flow of hydrogen}\left[\text{mol min}^{-1}\right] \times 2}{\text{total amount of hydrogen in the gas-phase products}} \times 100\% \quad (3)$$

The total amount of hydrogen in the gas-phase products was described as the sum of every product molar flow multiplied by the number of hydrogen atoms in a molecule.

The selectivity to carbon (carbon dioxide, carbon monoxide and alkanes) was determined as:

$$\text{Product selectivity}(\%) = \frac{\text{carbon in the product}}{\text{total amount of carbon in the gas-phase products}} \times 100\% \quad (4)$$

The total amount of carbon in the gas-phase products was calculated by summation of every identified product molar flow multiplied by the number of carbons in the molecule. The flow of carbon in a particular product and the total amount were defined in mol min^{-1}.

The specific platinum activity for the products was defined as:

$$\text{Specific catalytic activity} = \frac{\text{molar flow of the product (mol min}^{-1})}{\text{moles of Pt in the catalyst bed (mol)}} \quad (5)$$

Only platinum was taken into account in these calculations to compare the results in the current work with the data available in the literature for mainly platinum containing catalysts active in APR. The contribution of Pd to the catalytic activity of platinum is thus implicit by influencing predominantly formic acid decomposition.

3. Results and discussion

3.1. Catalyst characterization

The overall metal dispersion including both metals in the bimetallic catalyst was determined to be 47% by CO chemisorption.

A SEM image of the catalyst particles is presented in Fig. 2.

The surface composition was analysed by SEM–EDX. The catalyst surface was found to contain 4.8 wt% Pt and 1.3 wt% Pd, which is approximately two fold the nominal loading. This result can be explained by formation of the core–shell type catalyst with the outer surface of catalyst grains being thus enriched with the metals.

The TEM images are presented in Fig. 3 illustrating that the average metal cluster size is *ca.* 1.5 nm.

3.2. Experimental results

The experiments on the aqueous phase reforming of xylose or xylitol performed over a bimetallic Pt and Pd catalyst supported on mesoporous carbon were analyzed in terms of activity, selectivity, composition of alkanes and distribution of products in the liquid-phase. Totally, 46 compounds were identified and calibrated allowing a high degree of carbon identification.

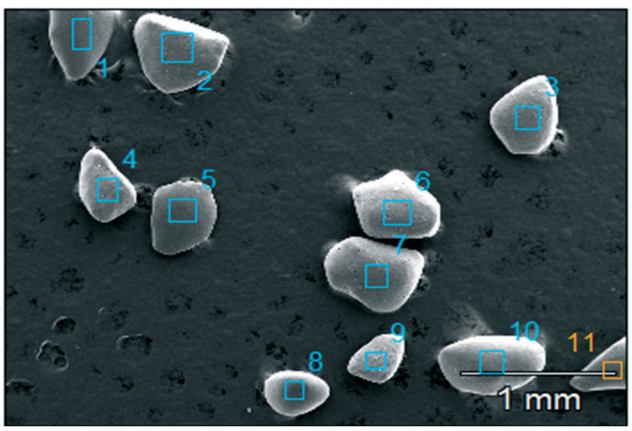

Fig. 2 SEM of the catalyst.

Experiments with xylose as the reactant were conducted at 175, 200 and 225 °C (Fig. 4). The APR of xylose at 225 °C resulted in clogging of the reactor in the absence of formic acid due to the formation of humins.

A complete conversion was obtained at 175 and 200 °C (Fig. 4A), however, most of the carbon remained in the liquid phase. At 175 °C *ca.* 20% of the total carbon was found in the gas-phase, while at 200 °C the amount increased to 40%. The total carbon balance closure was *ca.* 85% (Fig. 5A). H_2 and CO_2 were the main gaseous products detected (Fig. 4B) with, however, decreasing selectivity with time-on-stream (TOS), while the selectivity to alkanes increased during the experiments. Apparently, these results should be explained by catalyst inactivation when xylose was used as a substrate. The average specific platinum activity for H_2 formation was equal to 0.2 min^{-1} at 175 °C and 0.49 min^{-1} at 200 °C. In glucose APR it was reported previously that formation rates at 200 °C are equal to 0.11 min^{-1} (0.4 ml min^{-1} of hydrogen produced over 1 g of 3.26 wt% Pt/Al_2O_3).[47] These results illustrate an important difference between the sugars, *i.e. ca.* 5 times more productivity under the same conditions for xylose APR *vs.* glucose APR for similar catalysts.

Addition of formic acid to the xylose solution resulted in significant changes of the process. At 175 °C a decrease in conversion from 100% to 85% was noticed while formic acid exhibited a conversion of 59%. A similar behavior was observed for xylose and formic acid at 200 °C, while a further temperature increase resulted in complete conversion of both reactants. A decrease of formic acid decomposition was observed after two hours of TOS. At 175 °C, an increase in the gaseous products was detected accounting for 30% of the total carbon compared to 20% when no formic acid was present. The temperature increase resulted in more gaseous products, accounting for more than 50% of the products at 200 °C and 225 °C.

An interesting observation in Fig. 4 for APR of xylose in the presence of formic acid at 225 °C requiring further investigation is an increase of selectivity to hydrogen and CO_2 at the expense of selectivity towards alkanes. Such behavior cannot be directly related to catalyst inactivation evidenced through a decrease in formic acid decomposition, as a similar decline in activity for this decomposition under other conditions did not display the same selectivity increase.

It should be noted that despite changes in selectivity with TOS in the APR of xylose when formic acid was present in the feed, and a decline in formic acid conversion, the level of xylose conversion was rather stable (*e.g.* at 200 °C and 225 °C).

The qualitative product distribution was somewhat different in the presence and absence of formic acid. Fig. 4 shows that in APR of xylose in the absence of formic acid the selectivity to CO is very small similar to the results reported previously for xylitol APR.[14–18] These results are in line with the high water gas shift (WGS) activity of platinum catalysts under the reaction conditions favoring this reaction (*i.e.* reaction of carbon monoxide and steam giving carbon dioxide and hydrogen) in the forward direction. Interestingly

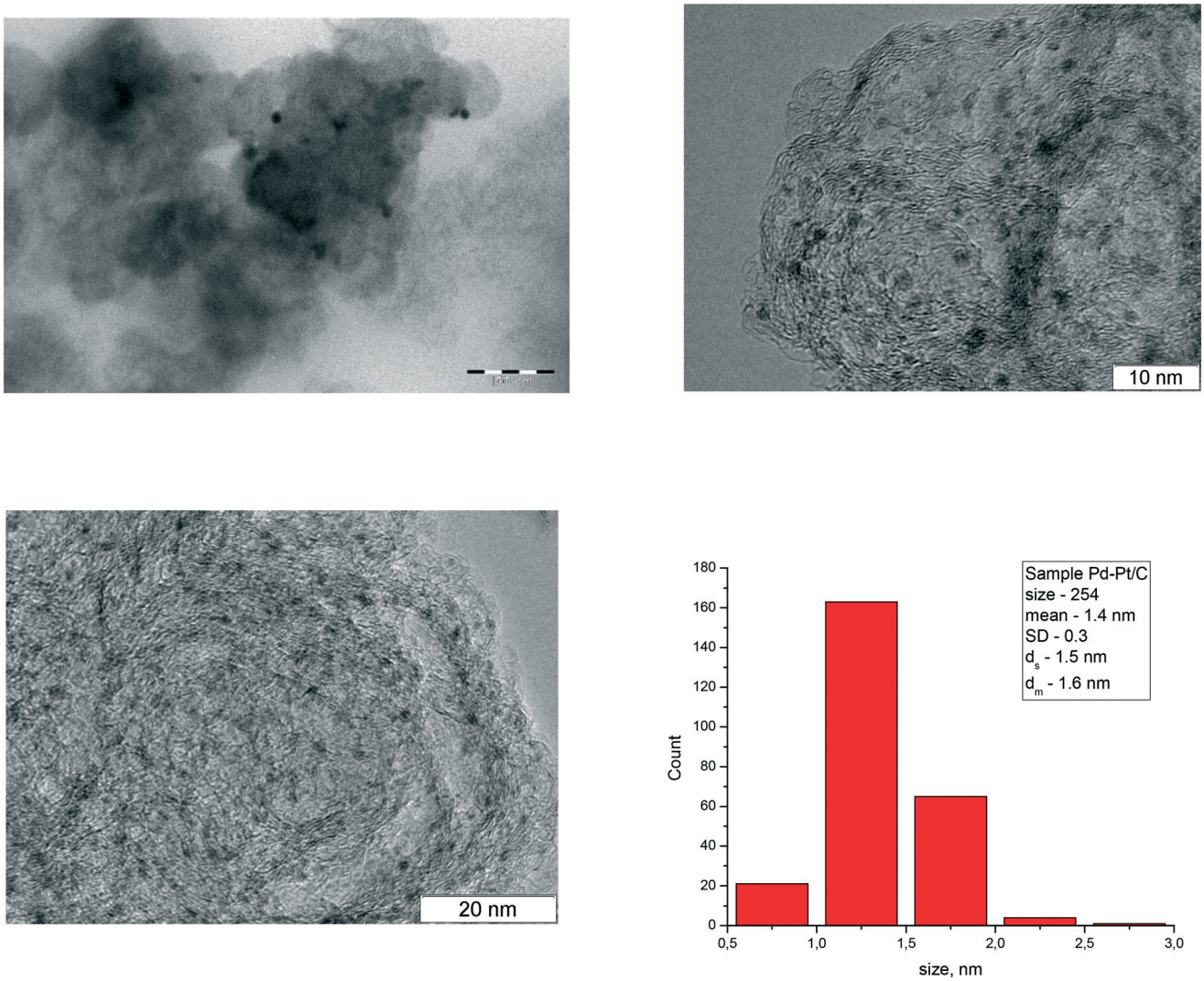

Fig. 3 TEM micrographs and the histogram of the catalyst.

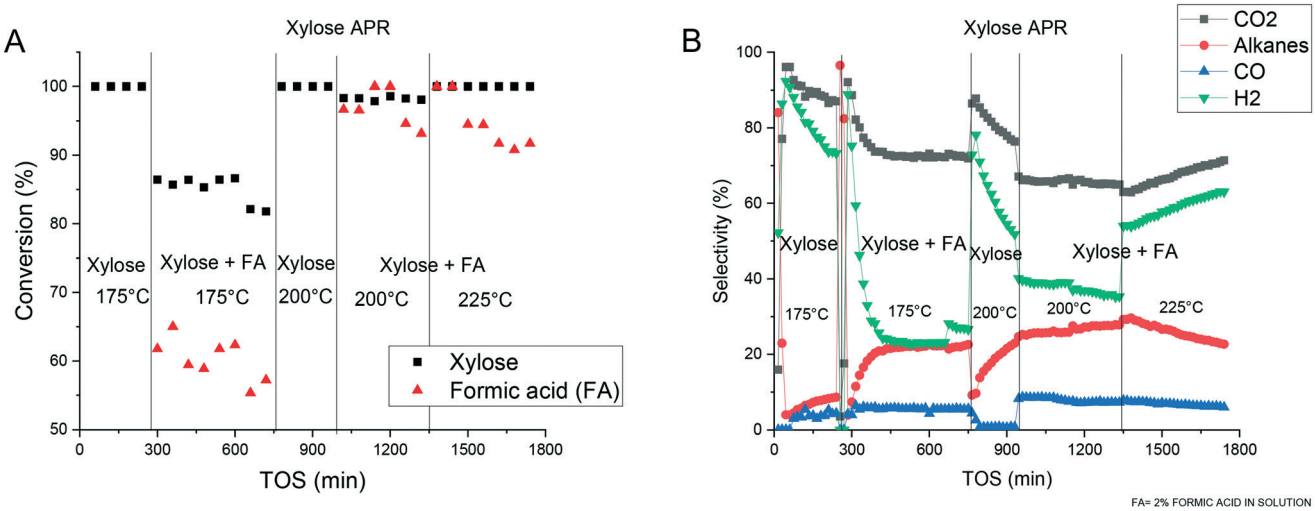

Fig. 4 Xylose APR: A) conversion and B) selectivity.

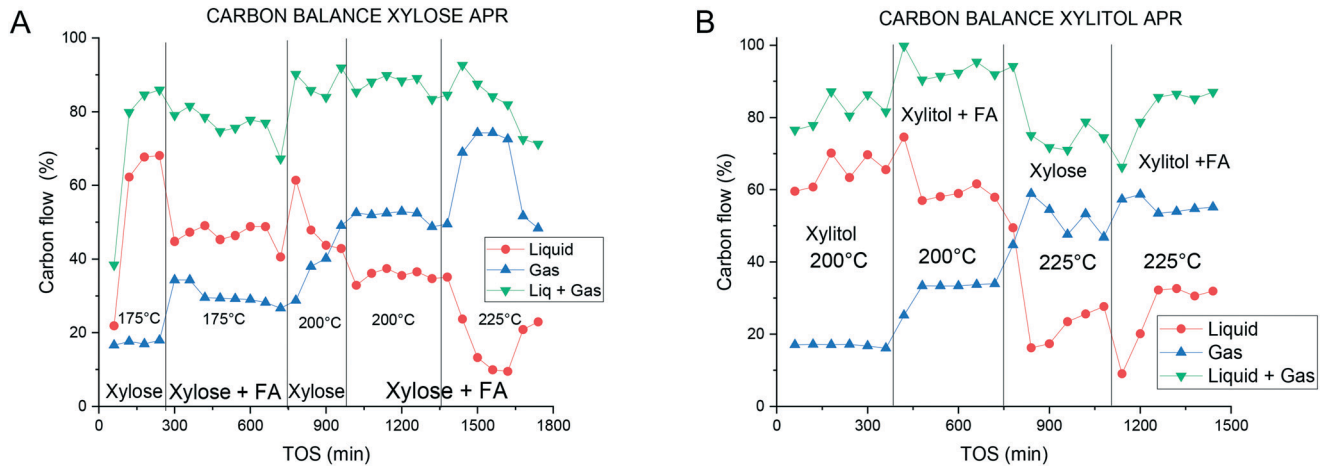

Fig. 5 Carbon balance in A) xylose and B) xylitol APR.

enough in the presence of formic acid there was a significant retardation of the water gas shift reaction.

The average specific platinum activity for hydrogen production at 175 °C, 200 °C and 225 °C was 0.04, 0.11 and 0.28 min^{-1}, respectively. A decrease in hydrogen production when formic acid was added compared to the xylose APR solution can be related to the transformation of xylose to furfural and humins already upstream the catalyst bed. These reactions have been addressed several times in the literature for different mixtures containing formic acid (*e.g.* xylose with formic acid and furfural with formic acid) for a similar temperature range.[48,49] According to Van Zandvoort *et al.*[50] under acidic conditions xylose can be completely converted at 180 °C giving a high yield of humins. It can also be speculated that higher than typical for APR of sugar alcohols the selectivity to CO observed in the current work is also connected with formation of humins.

The results presented above thus show that even in the presence of formic acid, which decomposition contributes to a reductive atmosphere, there is a clear decline in the gas yield with TOS (*e.g.* data in the presence of formic acid at 225 °C).

Apparently balancing of the rates for the APR with xylose, the decomposition of formic acid and generation of humins from xylose are key to successful xylose APR.

As an alternative to direct utilization of xylose in APR there could be an option to first hydrogenate xylose as such or in the presence of formic acid. It was thus instructive to study APR of xylitol. The latter displayed a behavior at 200 °C different from xylose APR, namely the conversion and selectivity towards gaseous products were lower than those for xylose, with 20% of carbon present in the gas phase. However, the selectivity to hydrogen and carbon dioxide was close to 100% (Fig. 6). An increase of the temperature to 225 °C resulted in the complete conversion of xylitol with 55% of the total carbon being present in the gas phase. However, an increase was observed in the alkane production (up to *ca.* 10%) with a similar decrease in the selectivity towards

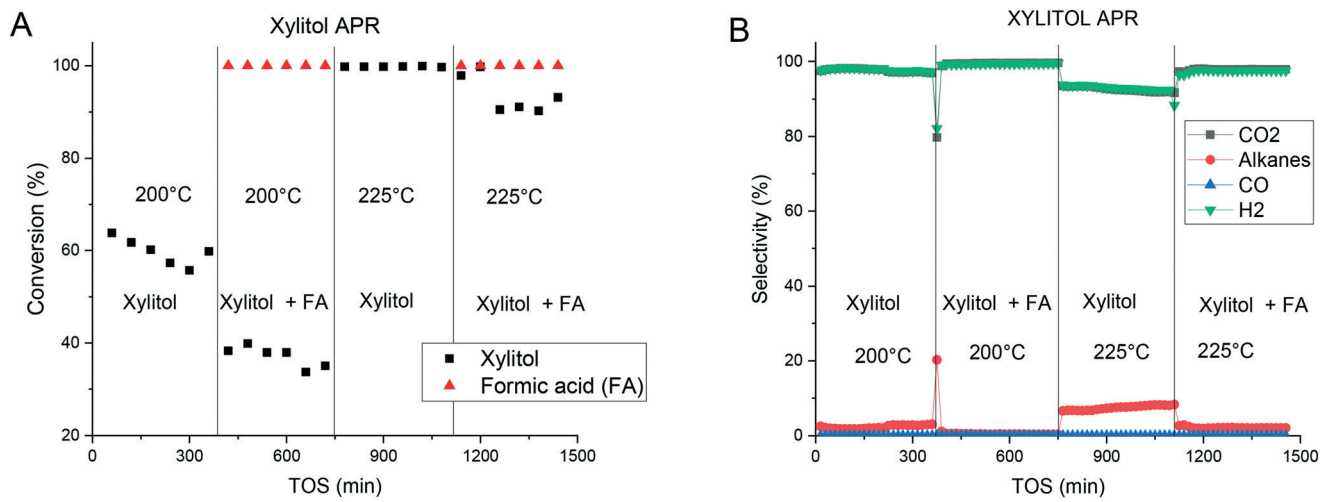

Fig. 6 Xylitol APR: A) conversion and B) selectivity.

hydrogen and carbon dioxide. The carbon balance and the product distribution in the liquid phase were similar to the APR of xylose (Fig. 5). The decrease in the activity was followed by an increase in the selectivity, which can be expressed as the specific activity for H_2 formation of 0.26 and 0.7 min^{-1} at 200 °C and 225 °C, respectively. These results are lower than those reported previously for 2.5% Pt/C at 225 °C,[14,15] however, the catalyst displayed a good stability compared to the literature findings not showing any activity decrease during the experiments.[14]

Experiments with the addition of formic acid to the reaction mixture showed a decrease in the xylitol conversion compared to pure xylitol solutions, while the formic acid conversion was complete at both 200 °C and 225 °C. Addition of formic acid resulted in an improved selectivity towards hydrogen decreasing the production of alkanes. This can be associated in part with efficient decomposition of formic acid over Pd in the presence of xylitol.

Such decomposition was also tested in the absence of xylitol. APR of a solution containing 1.5 wt% of formic acid was performed at 175 °C and 17 bar under the same gas flow but with a twofold higher liquid flow (*i.e.* 0.2 ml min^{-1}). Under these conditions efficient formic acid decomposition was observed resulting in 98.7% and stoichiometric quantities of only CO_2 and H_2 as products.

The selectivity towards gas-phase products increased as in the APR of xylose where the amount of carbon in the gas phase was increased after addition of formic acid. Hydrogen and CO_2 were the main gas-phase products. It should be noted that different to APR of xylose and in agreement with the previous work[14–18] no formation of CO was observed indicating an efficient water gas shift reaction.

The specific platinum activity for hydrogen formation was 0.46 and 0.84 min^{-1} at 200 °C and 225 °C, respectively. These results differ from those obtained in the APR of xylose in the presence of formic acid, displaying the opposite behavior with formic acid addition. For xylitol APR, addition of formic acid was instrumental in increasing the hydrogen production generating much less alkanes.

In the case of xylose APR (Fig. 4) addition of formic acid resulted thus in a decrease of conversion but an increase of selectivity to alkanes. An opposite behavior in terms of selectivity was observed for APR of xylitol (Fig. 6). Such observations show that the influence of formic acid cannot be explained just in terms of additional hydrogen generation in the presence of formic acid and its involvement in formation of alkanes. In contrast, the presence of formic acid besides influencing the transformations of xylose to furfural and humins discussed above, can also suppress dehydration of xylitol probably by adsorption on the same type of sites. Adsorption of xylose on the sites leading to alkanes through dehydration/hydrogenation should be thus less influenced by the presence of formic acid because of the carbonyl group, subsequently giving more alkanes.

While xylose was highly reactive under the experimental conditions, xylitol displayed lower conversion at lower temperatures. A comparison between Fig. 4B and 6B reveals significant differences in the selectivity as a function of TOS for the APR of xylose and xylitol. The selectivity towards hydrogen exceeded 90% and was stable for xylitol processing, while the selectivity ranged from 20 to 90% with xylose being much more unstable during the experiments apparently due to catalyst deactivation. However, xylose displayed a higher reactivity at lower temperature with the conversion being twofold at 200 °C compared to xylitol. This can be related to the APR mechanism of sugar alcohols requiring first the dehydrogenation to a corresponding aldehyde.[14,16]

4. Selectivity to alkanes

The distribution of alkanes in the APR of xylose was dependent on the reaction conditions (Fig. 7A). At 200 °C alkanes with smaller carbon chains (C1–C3) were mainly generated with propane being the most prominent exhibiting 6% selectivity. However, under all other conditions, the most important alkanes had five and six carbon atoms. The presence of hydrocarbons with a chain length larger than in the reactants has been also previously observed[14,17] and can be explained by condensation reactions.

The APR of xylitol (Fig. 7B) exhibited a low selectivity to alkanes compared with xylose. The distribution did not change with temperature or addition of formic acid, but C1 and C2 alkanes remain the most prominent products. It should be noted that when formic acid was added, the overall selectivity to alkanes was lower. Moreover, the selectivity to alkanes was lower compared with the values reported previously[14,15] where C1–C3 were the most abundant products.

In general, the presence of methane and ethane was significant in the APR of xylitol while the yields of C3 products were lower. The APR of xylose resulted in propane followed by ethane with less methane formation in the experiments conducted in the absence of formic acid. Introduction of formic acid shifted the selectivity among the alkanes predominantly to C5 and C6 compounds in the APR of xylose. The APR mechanism of sugar alcohols[14] assumes two main parallel routes, *i.e.* through dehydrogenation and decarbonylation or dehydration/hydrogenation. The latter pathway is responsible for the formation of alkanes. Apparently, the presence of formic acid in the reaction mixture and its decomposition to hydrogen and carbon dioxide influenced the main transformation pathways in APR of xylose.

5. Liquid-phase composition

A high amount of intermediates was observed in the liquid phase for the APR of xylose (Fig. 8A) with the maximum concentration reaching 0.04 M for methanol and propanediols. Similar to the distribution of alkanes, the liquid phase was clearly influenced by the reaction conditions. However, the most important products were those with C2 and C3 carbon atoms.

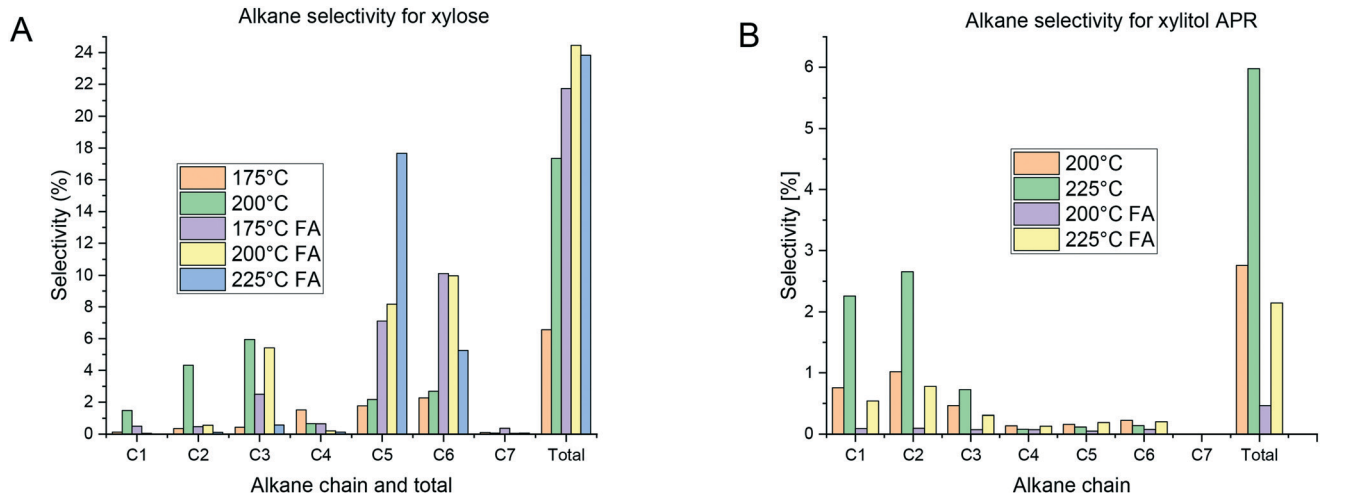

Fig. 7 Alkane selectivity in APR of A) xylose and B) xylitol.

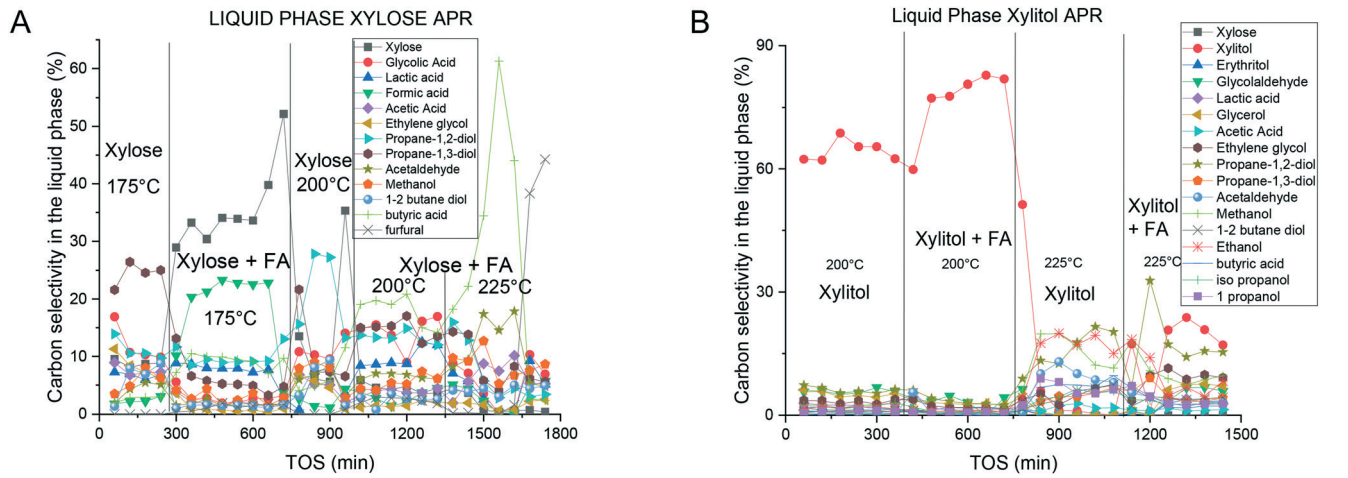

Fig. 8 Distribution of the liquid phase products in the APR of A) xylose and B) xylitol.

As mentioned above mechanistic studies of APR of sugar alcohols[14–18] suggest dehydrogenation of the alcohol to the corresponding aldehyde followed by decarbonylation as the first steps along the route giving eventually carbon dioxide and water. In this context, it is not surprising that APR of xylose did not result in formation of xylitol.

In the case of the APR of xylitol, the liquid phase (Fig. 8B) contained compounds in concentrations similar to the APR of xylose, with methanol being the most abundant. Not surprisingly, xylose was also present in the reaction mixture. With increased temperature, higher amounts of liquid-phase products were observed in the APR of xylitol compared to the APR of xylose. As expected the amount of the liquid phase products decreased with increasing temperature. The presence of furfural in some samples suggests multistep dehydration of xylose. Previously numerous intermediates have been reported for xylitol APR.[51] A high level of carbon identification expressed in the carbon balance (Fig. 5) displays a good identification of the main reaction products.

The liquid-phase compositions during the APR of xylose and xylitol exhibited only small changes when formic acid was added to the feed. The product mixtures had similar compositions, with methanol and propanediols exhibiting the highest concentrations for both substrates.

6. Mechanistic aspects of xylose and xylitol APR

Despite important differences between the APR of xylose and xylitol, most of the liquid and gas phase products were the same suggesting similar overall reaction mechanisms and pathways.

In the APR of xylose, the liquid phase exhibited a rather constant product distribution with most of the products having two or three carbon atoms showing a cleavage of the substrate molecules. This behavior was also observed in the gas phase as significant amounts of C2 and C3 alkanes were detected. Neira D'Angelo *et al.*[52] described a similar route for

glycerol production from sorbitol due to C–C hydrogenolysis in APR.

However, the gas-phase mainly contained significant amounts of C5 and C6 alkanes. This behavior could be due to hydrogenolysis of C–O bonds and dehydration of the substrate, as described by Godina *et al.*[53] However, the presence of longer alkanes should be related to condensation reactions. Such reactions were more prominent after addition of formic acid.

The APR of xylitol under different conditions produced mainly C1–C3 products in both phases. These results are similar to the xylose APR, however, a high amount of C1 products indicates a further cleavage of the C–C bonds.

The presence of similar products in the xylose and xylitol APR suggests similarities in the reaction mechanisms for both substrates. However, the structure of the substrate has a significant influence on the hydrogen selectivity and the catalyst stability. The presence of a carbonyl group in the chain results in a high activity of the substrate at the expense of the selectivity towards hydrogen, which requires careful process control and a separation step after the APR of xylose. Formic acid used typically in reactive extraction of hemicellulosic sugars from biomass can be efficiently converted to hydrogen with APR, however, complete *in situ* hydrogenation of the sugars to sugar alcohols prior to hydrogen production was not achieved, as APR of xylose was different from APR of a xylitol and formic acid mixture.

Subsequently hydrogenation of xylose to xylitol after reactive extraction of hemicelluloses (*e.g.* xylan) in the presence of formic acid should be done upstream APR of xylitol. Overall feasibility of this approach requires a detailed techno-economic analysis of each step, similar to what was done for APR of xylitol.[17] Such work is currently in progress.

7. Conclusions

Aqueous phase reforming of xylose and xylitol was performed over a bimetallic Pt/Pd catalyst supported on mesoporous carbon Sibunit. The experiments were conducted in a laboratory scale packed bed reactor in the temperature range of 175 to 225 °C at a constant pressure of 32 bar. In total, 48 compounds were identified and quantified.

The APR of xylitol displayed a high selectivity to hydrogen and carbon dioxide with close to 100% conversion at the highest experimental temperature (225 °C). The xylose APR displayed close to complete conversions at all reaction temperatures, however, the selectivity was significantly lower than that for the APR of xylitol. A decrease in the selectivity was also observed during the experiments.

Addition of formic acid, mimicking the APR of an industrially relevant feedstock obtained from reactive extraction of hemicellulosic sugar from biomass resulted in the decrease of the hydrogen selectivity for xylose APR, but an increase in selectivity when xylitol was used as the substrate. Formic acid was efficiently converted to hydrogen.

The carbon content in the gas phase increased with temperature for both xylose and xylitol. Moreover, addition of formic acid generated an increase in the amount of gas-phase products resulting in more extensive formation of alkanes from xylose and more CO_2 in the APR of xylitol.

The alkane distribution in the APR of xylose depended on the reaction conditions. However, C5 and C6 alkanes were typically the most abundant hydrocarbons. In the APR of xylitol, the product distribution was rather constant and most of the observed alkanes were C1–C2 alkanes.

The liquid-phase product distributions were similar for xylose and xylitol with methanol and propanediols being the most prominent ones. In general, the concentrations of the liquid-phase products were rather low.

The results indicated that xylitol and mixtures of xylitol and formic acid can successfully be converted to renewable hydrogen with a high conversion and high selectivity by applying aqueous phase reforming over a bimetallic Pt/Pd catalyst.

Conflicts of interest

There are no conflicts of interest.

Acknowledgements

The authors are grateful to L. Silvander (Åbo Akademi University) for SEM analysis. Financial support was provided by Business Finland through the project: biohydrogen from wood hemicellulose hydrolysate. Catalyst synthesis was supported by RFBR Grant 18-53-45013 IND_a and TEM analysis was supported by the Ministry of Science and Higher Education of the Russian Federation (project AAAA-A17-117041710075-0).

References

1 R. Cortright, R. Davda and J. Dumesic, Hydrogen from catalytic reforming of biomass-derived hydrocarbons in liquid water, *Nature*, 2002, **418**, 964–967.
2 N. Taccardi, D. Assenbaum, M. Berger, A. Bösmann, F. Enzenberger, R. Wölfel, S. Neuendorf, V. Goeke, N. Schödel, H. Maass, H. Kistenmacher and P. Wasserscheid, Catalytic production of hydrogen from glucose and other carbohydrates under exceptionally mild reaction conditions, *Green Chem.*, 2010, **12**, 1150–1156.
3 B. Meryemoglu, S. Irmak, A. Hasanoglu, O. Erbatur and B. Kaya, Influence of particle size of support on reforming activity and selectivity of activated carbon supported platinum catalyst in APR, *Fuel*, 2014, **134**, 354–357.
4 B. Meryemoglu, A. Hesenov, S. Irmak, O. Atanur and O. Erbatur, Aqueous-phase reforming of biomass using various types of supported precious metal and RANEY®-nickel catalysts for hydrogen production, *Int. J. Hydrogen Energy*, 2010, **35**, 12580–12587.
5 S. Irmak, B. Meryemoglu, A. Hasanoglu and O. Erbatur, Does reduced or non-reduced biomass feed produce more gas in aqueous-phase reforming process?, *Fuel*, 2015, **139**, 160–163.

6 R. Davda, J. Shabaker, G. Huber, R. Cortright and J. Dumesic, A review of catalytic issues and process conditions for renewable hydrogen and alkanes by aqueous-phase reforming of oxygenated hydrocarbons over supported metal catalysts, *Appl. Catal., B*, 2005, **56**, 171–186.

7 I. Coronado, M. Stekrova, M. Reinikainen, P. Simell, L. Lefferts and J. Lehtonen, A review of catalytic aqueous-phase reforming of oxygenated hydrocarbons derived from biorefinery water fractions, *Int. J. Hydrogen Energy*, 2016, **41**, 11003–11032.

8 P. Vaidya and J. Lopez-Sanchez, Review of hydrogen production by catalytic aqueous-phase reforming, *ChemistrySelect*, 2017, **2**, 6563–6576.

9 M. Valenzuela, C. Jones and P. Agrawal, Batch aqueous-phase reforming of woody biomass, *Energy Fuels*, 2006, **20**, 1744–1752.

10 X. Wang, N. Li, L. Pfefferle and G. Haller, Pt–Co bimetallic catalyst supported on single walled carbon nanotube: XAS and aqueous phase reforming activity studies, *Catal. Today*, 2009, **14**, 160–165.

11 T. Kim, H. Kim, K. Jeong, H. Chae, S. Jeong, C. Leeb and C. Kim, Catalytic production of hydrogen through aqueous-phase reforming over platinum/ordered mesoporous carbon catalysts, *Green Chem.*, 2011, **13**, 1718–1728.

12 B. Meryemoglu, A. Hesenov, S. Irmak, O. Atanur and O. Erbatur, Aqueous-phase reforming of biomass using various types of supported precious metal and RANEY®-nickel catalysts for hydrogen production, *Int. J. Hydrogen Energy*, 2010, **35**, 12580–12587.

13 T. Jiang, T. Wang, L. Ma, Y. Li, Q. Zhang and X. Zhang, Investigation on the xylitol aqueous-phase reforming performance for pentane production over Pt/HZSM-5 and Ni/HZSM-5 catalysts, *Appl. Energy*, 2012, **90**, 51–57.

14 L. Godina, A. Kirilin, A. Tokarev, I. Simakova and D. Y. Murzin, Sibunit-supported mono- and bimetallic catalysts used in aqueous-phase reforming of xylitol, *Ind. Eng. Chem. Res.*, 2018, **57**, 2050–2067.

15 A. Kirilin, B. Hasse, A. Tokarev, L. Kustov, G. Baeva, G. Y. Bragina, A. Stakheev, A. Rautio, T. Salmi, B. Etzold, J.-P. Mikkola and D. Y. Murzin, Aqueous-phase reforming of xylitol over Pt/C and Pt/TiC-CDC catalysts: catalyst characterization and catalytic performance, *Catal. Sci. Technol.*, 2014, **4**, 387–401.

16 A. Kirilin, A. Tokarev, H. Manyar, C. Hardacre, T. Salmi, J.-P. Mikkola and D. Y. Murzin, Aqueous phase reforming of xylitol over Pt-Re bimetallic catalyst: Effect of the Re addition, *Catal. Today*, 2014, **223**, 97–107.

17 D. Y. Murzin, S. Garcia, V. Russo, T. Kilpiö, L. Godina, A. Tokarev, A. Kirilin, I. Simakova, S. Poulston, D. Sladkovskiy and J. Wärna, Kinetics, modeling, and process design of hydrogen production by aqueous phase reforming of xylitol, *Ind. Eng. Chem. Res.*, 201, **56**, 13240–13253.

18 A. Kirilin, A. Tokarev, L. Kustov, T. Salmi, J.-P. Mikkola and D. Y. Murzin, Aqueous phase reforming of xylitol and sorbitol: Comparison and influence of substrate structure, *Appl. Catal., A*, 2012, **435**, 172–180.

19 T. Jiang, Q. Zhang, T. Wang, Q. Zhang and L. Ma, High yield of pentane production by aqueous-phase reforming of xylitol over Ni/HZSM-5 and Ni/MCM22 catalysts, *Energy Convers. Manage.*, 2012, **59**, 58–65.

20 T. Kim, H. Park, Y. Yang, S. Jeong and C. Kim, Hydrogen production via the aqueous phase reforming of polyols over three dimensionally mesoporous carbon supported catalysts, *Int. J. Hydrogen Energy*, 2014, **39**, 11509–11516.

21 H. Duarte, M. Sad and C. Apesteguía, Production of bio-hydrogen by liquid processing of xylitol on Pt/Al_2O_3 catalysts: Effect of metal loading, *Int. J. Hydrogen Energy*, 2017, **42**, 4051–4060.

22 S. Narayanan, J. Vijaya, S. Sivasanker, T. Sankaranarayanan, C. Ragupathi, L. Kennedy, R. Jothiramalingam, H. Al-Lohedan and A. Tawfeek, Catalytic conversion of polyols (sorbitol and xylitol) to hydrocarbons over hierarchical ZSM-5 zeolite catalysts in a fixed bed reactor, *React. Kinet., Mech. Catal.*, 2017, **122**, 247–257.

23 R. Ripken, J. Meuldijk, J. Gardeniers and S. Le Gac, Influence of the water phase state on the thermodynamics of aqueous-phase reforming for hydrogen production, *ChemSusChem*, 2017, **10**, 4909–4913.

24 A. Fasolini, R. Cucciniello, E. Paone, F. Mauriello and T. Tabanelli, A short overview on the hydrogen production via aqueous phase reforming (APR) of cellulose, C6-C5 sugars and polyols, *Catalyst*, 2019, **9**, 917.

25 G. Pipitone, G. Zoppi, A. Frattini, S. Bocchini, R. Pirone and S. Bensaid, Aqueous phase reforming of sugar-based biorefinery streams: from the simplicity of model compounds to the complexity of real feeds, *Catal. Today*, 2020, **345**, 267–279.

26 A. Kirilin, J. Wärna, A. Tokarev and D. Y. Murzin, Kinetic modeling of sorbitol aqueous-phase reforming over Pt/Al_2O_3, *Ind. Eng. Chem. Res.*, 2014, **53**, 4580–4588.

27 S. Dapía, V. Santos and J. C. Parajó, Study of formic acid as an agent for biomass fractionation, *Biomass Bioenergy*, 2002, **22**, 213–221.

28 M. Zhang, W. Qi, R. Liu, R. Su, S. Wu and Z. He, Fractionating lignocellulose by formic acid: Characterization of major components, *Biomass Bioenergy*, 2010, **34**, 525–532.

29 J. Snelders, E. Dornez, B. Benjelloun-Mlayah, W. Huijgen, J. de Wild, R. Gosselink, J. Gerritsma and C. Courtin, Biorefining of wheat straw using an acetic and formic acid based organosolv fractionation process, *Bioresour. Technol.*, 2014, **156**, 275–282.

30 A. Cesaro, A. Conte, H. Carrère, E. Trably, F. Paillet and V. Belgiorno, Formic acid pretreatment for enhanced production of bioenergy and biochemicals from organic solid waste, *Biomass Bioenergy*, 2020, **133**, 105455.

31 J. Villaverde, J. Li, M. Ek, P. Ligero and A. de Vega, Native lignin structure of Miscanthus x giganteus and its changes during acetic and formic acid fractionation, *J. Agric. Food Chem.*, 2009, **57**, 6262–6270.

32 X. Jian, M. Thomsen and A. Thomsen, Pretreatment on corn stover with low concentration of formic Acid, *J. Microbiol. Biotechnol.*, 2009, **19**, 845–850.

33 M. Li, S. Yang and R. Sun, Recent advances in alcohol and organic acid fractionation of lignocellulosic biomass, *Bioresour. Technol.*, 2016, **200**, 971–980.
34 K. Tedsree, T. Li, S. Jones, C. Chan, K. Yu, P. Bagot, E. Marquis, G. Smith and S. Tsang, Hydrogen production from formic acid decomposition at room temperature using a Ag–Pd core–shell nanocatalyst, *Nat. Nanotechnol.*, 2011, **6**, 302–307.
35 C. Fellay, P. Dyson and G. Laurenczy, A viable hydrogen-storage system based on selective formic acid decomposition with a ruthenium catalyst, *Angew. Chem., Int. Ed.*, 2008, **47**, 3966–3968.
36 D. Bulushev, S. Beloshapkin and J. Ross, Hydrogen from formic acid decomposition over Pd and Au catalysts, *Catal. Today*, 2010, **154**, 7–12.
37 Q. Bi, X. Du, Y. Liu, Y. Cao, H. He and K. Fan, Efficient subnanometric gold-catalyzed hydrogen generation via formic acid decomposition under ambient conditions, *J. Am. Chem. Soc.*, 2012, **134**, 8926–8933.
38 J. Yu and P. Savage, Decomposition of formic acid under hydrothermal conditions, *Ind. Eng. Chem. Res.*, 1998, **37**, 2–10.
39 J. Yoo, F. Abild-Pedersen, J. Nørskov and F. Studt, Theoretical analysis of transition-metal catalysts for formic acid decomposition, *ACS Catal.*, 2014, **4**, 1226–1233.
40 G. Huber, J. Shabaker, S. Evans and J. Dumesic, Aqueous-phase reforming of ethylene glycol over supported Pt and Pd bimetallic catalysts, *Appl. Catal., B*, 2006, **62**, 226–235.
41 A. Soares, H. Atia, U. Armbruster, F. Passos and A. Martin, Platinum, palladium and nickel supported on Fe_3O_4 as catalysts for glycerol aqueous-phase hydrogenolysis and reforming, *Appl. Catal., A*, 2017, **548**, 179–190.
42 J. Liu, B. Sun, J. Hu, Y. Pei, H. Li and M. Qiao, Aqueous-phase reforming of ethylene glycol to hydrogen on Pd/Fe_3O_4 catalyst prepared by co-precipitation: Metal–support interaction and excellent intrinsic activity, *J. Catal.*, 2010, **274**, 287–295.
43 L. Godina, A. Tokarev, I. Simakova, P. Mäki-Arvela, E. Kortesmäki, J. Gläseld, L. Kronberg, B. Etzold and D. Y. Murzin, Aqueous-phase reforming of alcohols with three carbon atoms on carbon supported Pt, *Catal. Today*, 2018, **301**, 78–89.
44 B. Kabyemela, T. Adschiri, R. Malaluan and K. Arai, Kinetics of glucose epimerization and decomposition in subcritical and supercritical water, *Ind. Eng. Chem. Res.*, 1997, **36**, 1552–1558.
45 B. Kabyemela, T. Adschiri, R. Malaluan, K. Arai and H. Ohzeki, Rapid and selective conversion of glucose to erythrose in supercritical water, *Ind. Eng. Chem. Res.*, 1997, **36**, 5063–5067.
46 B. Kabyemela, T. Adschiri, R. Malaluan and K. Arai, Glucose and fructose decomposition in subcritical and supercritical water: Detailed reaction pathway, mechanisms, and kinetics, *Ind. Eng. Chem. Res.*, 1999, **38**, 2888–2895.
47 A. Tanksale, J. Beltramini and G. Lu, Reaction mechanisms for renewable hydrogen from liquid phase reforming of sugar compounds, *Dev. Chem. Eng. Miner. Process.*, 2006, **14**, 9–18.
48 K. Lamminpää, J. Ahola and J. Tanskanen, Kinetics of furfural destruction in a formic acid medium, *RSC Adv.*, 2014, **4**, 60243–60248.
49 K. Lamminpää, J. Ahola and J. Tanskanen, Kinetics of xylose dehydration into furfural in formic acid, *Ind. Eng. Chem. Res.*, 2012, **51**, 6297–6303.
50 I. Van Zandvoort, Y. Wang, C. Rasrendra, E. Van Eck, P. Bruijnincx, H. Heeres and B. Weckhuysen, Formation, molecular structure, and morphology of humins in biomass conversion: Influence of feedstock and processing conditions, *ChemSusChem*, 2013, **6**, 1745–1758.
51 A. Kirilin, A. Tokarev, E. Murzina, L. Kustov, J.-P. Mikkola and D. Y. Murzin, Reaction products and transformations of intermediates in the aqueous-phase reforming of sorbitol, *ChemSusChem*, 2010, **3**, 708–718.
52 M. Neira D'Angelo, V. Ordomsky, J. Van der Schaaf, J. Schouten and T. Nijhuis, Aqueous phase reforming in a microchannel reactor: the effect of mass transfer on hydrogen selectivity, *Catal. Sci. Technol.*, 2013, **3**, 2834–2842.
53 L. Godina, A. Kirilin, A. Tokarev and D. Y. Murzin, Aqueous phase reforming of industrially relevant sugar alcohols with different chiralities, *ACS Catal.*, 2015, **5**, 2989–3005.